Holographic Direct View Display
From Light Field Recording to Phase Only Hologram

Stephen Hamann Xuerong Xiao

Abstract

The light field is a 4D recording that includes the positional and directional information for incoming rays of an image. A hologram is a recording that reconstructs the complex wavefront of an image to include parallex and depth cues. We relate these two concepts using the Wigner distribution, and attempt to recreate a light field recorded scene using a phase only hologram.

1. Introduction

There exists a developing interest in wearable and 3D displays. Practically every major technological company is becoming involved in the development of these devices. Holographic displays seem to be an ideal modality for the future of these products. In this report, we discuss our project to utilize a light field recording to display a hologram on a Holoeye PLUTO Liquid Crystal on Silicon (LCoS) phase only Spatial Light Modulator (SLM). This hologram can be seen by direct view or by projection onto a screen. We believe that this project is novel in taking a recorded light field using the commercially available Lytro Illum all the way to displaying an actual viewable hologram.

1.1. Light Field

A light field is a 4D function that describes geometric light rays at every point in space travelling from every direction. One of the common ways to parameterize a light field is to use two parallel planes, such as the lenslet plane and the detector plane in a light field camera. A light field camera has a lenslets array at the image plane of the primary lens system, and a detectors array at the image plane of the lenslets. The lenslets array images the exit pupil of the primary lens system, and one lenslet corresponds to one pixel in the image. The detector elements associated with a lenslet measures the intensity of light rays arriving from different directions at that lenslet. Therefore, the light field camera generates information with both positional intensities and positional ray angles.

1.2. Holography

A traditional hologram is the recording of the interference between a coherent light source reflected off of a scene and another nonscattered reference beam from the same source. This interference pattern creates fringes that diffract light in such a way as to recreate the scene perfectly in the far field. Perfect recreation means that a human's eyes cannot tell the difference without context between a hologram and a window into the scene in real life due to the hologram's depth cues and parallex. For digital holography, these interference patterns can be recorded or simulated, and then attempted to be replicated using a light modulator. Alternatively, we can view the fringes as a recording of the complex signal and attempt to recreate the phase and amplitude of the electromagnetic wave. For the project, we will be taking the latter approach for reconstruction.

1.3. Why use light field for holography?

Both the light field and the hologram include positional intensity and directionality. More importantly, the light field like a hologram contains depth cues from the directional information. This fact is readily seen in the Illum's ability to refocus the image to different depths of focus. For a fixed perspective direct view display, this depth information is much more important than the parallex, which requires much higher spatial frequency information. In general, a holographic recording will always be better than a light field for holographic reconstruction. However, a light field recording can be incoherent and does not require a reference. Therefore, any light source, even natural light, can be used, and so capturing light fields is much easier and more flexible than the interformetric recording required for a hologram.

2. Related Work

We are not the first to recognize the connection between holography and light field imaging. Ziegler of ETH Zurich developed a transformation in 2007 that invovlved creating a depth map and 3D rendering to switch between the light field and the hologram using computer generated holographic techniques [1]. This method has compelling results,

but it is computationally strenuous. Also, the demonstration was made using a hand captured light field by taking multiple images rather than a plenoptic camera, so it is hard to compare to our results.

We will be using the relationship between the Wigner distribtuion and the light field as discussed by Zhang and Levoy in 2009 [2] and Goodman in 2013 [3]. The Wigner distribution W for some complex signal V [1] is defined by Goodman as:

$$W_V(x,u) = \int_{-\infty}^{\infty} V(x+\frac{x'}{2})V^*(x-\frac{x'}{2})\exp(-i2\pi x'u)dx' \tag{1}$$

The Wigner distribution displays a complex signal and its Fourier information in the same 4D function. It is real valued, though it can be negative. The Wigner is a useful tool in optics, since near field diffraction can be calculated using a simple shear and the Frauenhofer (Fourier) transform of the field is a simple quarter rotation. However, it also bears a lot of similarity to the light field. Both are 4D and the spatial frequency information of the Wigner can be equated to the sub-pixel information from the light field. In fact, Zhang shows that the relationship between the light field and Wigner is a simple blur and axial change. The relationship between the Lytro Illum recording $l_{discrete}$ and the Wigner distribution W of some coherent signal T with wavelength $lambda$ is thus [2]:

$$l_{discrete}[m,n,p,q] = sample\left(W_T(-x,-y,\frac{u}{\lambda},\frac{v}{\lambda}) \otimes P(\frac{u}{\lambda},\frac{v}{\lambda})\right) \tag{2}$$

where P is the blurring prefilter from the microlens aperture, x and y are the real space coordinates and u and v are the reciprocal coordinates, and m, n, p and q are the non-rectified pixel coordinate of the discrete light field with m and n equivalent to real space coordinates and p and q equivalent to the reciprocal coordinates.

3. Method

We first calculate the complex wavefront captured by the light field, and then attempt to reconstruct it using an optimized phase hologram.

3.1. From light field to hologram

First we take the rectified light field image and convert it to its 4D form. Our Wigner function $W[m,n,p,q]$ is taken to be the same as the 4D light field, with m,n,p and q as described above. Ideally we need to correct for the Wigner prefilter caused by the microlens aperture. However, we do not know the exact specifications of the microlens array and guessing the prefilter would not be useful. The real space x and y axis vectors are calculated using the pixel pitch times the number of pixels per microlens. The spatial frequency $\mathbf{k}$ vectors are calculated from the center of pixel ray direction in spherical coordinates:

$$k_x = \frac{2\pi}{\lambda}\cos\theta\sin\phi \tag{3}$$

$$k_y = \frac{2\pi}{\lambda}\sin\theta sin\phi \tag{4}$$

where θ is the axial ray direction and ϕ is the azimuthal direction. These axes are treated as vectors that share the size as the Wigner matrix dimensions.

From Lohmann [4], the original complex signal with some complex constant can be calculated from a Wigner function by taking the inverse Fourier transform of the Wigner with the continuous axis scaled. Since we are using a discrete non-symmetric matrix, we can ignore the axis scaling and normalize over peak intensity to deal with the complex constant. We therefore calculate our complex wavefront $U[m,n]$ as:

$$U[m,n] = \sum_p \sum_q W[m,n,p,q]\exp\left\{i2\pi\left(x[m]k_x[p] + y[n]k_y[q]\right)\right\} \tag{5}$$

3.2. Phase-only hologram optimization

The complex image with both amplitude and phase needs to be optimized to a phase-only Fourier hologram, in order to be displayed on a phase-only spatial-light modulator. Let $h(\phi)$ be a function of phase ϕ, U the target complex matrix from the Wigner distribution function, and J the objective function to be minimized. The optimization problem can be described as:

$$\text{minimize } J = \frac{1}{2N}\sum_{u,v}\|\mathcal{F}\left\{h(\phi_{st})\right\} - U\|^2 \tag{6}$$

$$\text{subject to } |h(\phi_{st})| = 1, \tag{7}$$

where N is the number of pixels in the complex image U, u-v plane is where U locates, and s-t plane is where the hologram locates. The pure phase function can also be writen as $h(\phi) = \exp(i\phi)$.

We implemented gradient descent to update phase ϕ in each iteration:

$$\phi := \phi - \alpha\frac{\partial J}{\partial \phi}, \tag{8}$$

where α is the learning rate and can be determined by trial-and-error. The rate should be sufficiently small to achieve

[1] The given equation is for a 1D signal, resulting in a 2D Wigner distribution. A 2D image will result in a 4D Wigner distribution.

convergence, but if it is too small, gradient descent can be slow to converge.

By taking the partial derivative and manipulating the real and imaginary part of each term, we have:

$$\frac{\partial J}{\partial \phi_{st}} = \frac{1}{N} \Im \left\{ \exp\left(-i\phi_{st}\right) \sum_{u,v} F^*_{stuv} \Delta_{uv} \right\}, \quad (9)$$

where F is the DFT tensor, F_{stuv} is one of the elements in the tensor, and

$$\begin{aligned} \Delta_{uv} &= \left(\mathcal{F}\left\{h(\phi_{st})\right\} - U\right)_{uv} \\ &= \sum_{s,t} F_{stuv} \exp\left(i\phi_{st}\right) - U_{uv}. \end{aligned} \quad (10)$$

Since F is unitary, we have $FF^\dagger = \mathbb{I}$, and Equation (9) becomes

$$\frac{\partial J}{\partial \phi_{st}} = \frac{1}{N} \Im \left\{ F^\dagger \left[\Delta_{uv} \exp\left(-i\phi_{st}\right) \right] \right\}, \quad (11)$$

where $F^\dagger$ corresponds to ifft2 in MATLAB. We implement the pixel-wise summing operation using the fast Fourier transform (FFT) algorithm to reduce the number of computations. The final update equation becomes:

$$\phi \coloneqq \phi - \frac{\alpha}{N} \Im \left\{ F^\dagger \left[\Delta_{uv} \exp\left(-i\phi\right) \right] \right\}, \quad (12)$$

which can be interpreted as a weighted back-propagation of field from u-v plane to s-t plane.

Instead of comparing the Fourier transform of a pure phase function to the complex image, we could also compare the pure phase function to the inverse Fourier transform of the complex image. In this case, the optimization problem can be formulated as:

$$\text{minimize } \; J = \frac{1}{2N} \sum_{u,v} \left\| h(\phi_{st}) - \mathcal{F}^{-1}\{U\} \right\|^2 \quad (13)$$

$$\text{subject to } \; |h(\phi_{st})| = 1, \quad (14)$$

This formulation gives rise in simpler mathematical manipulations but with less optimal results. Intuitively, the first method incorporates the interactions of pixels starting from the hologram plane as light propagates to the far field, whereas the second method optimizes each pixel individually. As shown in Figure 1, P represents a target point to be optimized, and P' is the point on the unit circle that is closest to P. The optimization in the second method moves P close to P'. Hence it is only optimizing the magnitude, but not the phase of the complex image. So the optimization will simply converge to the phase of the Fourier transform of the complex signal.

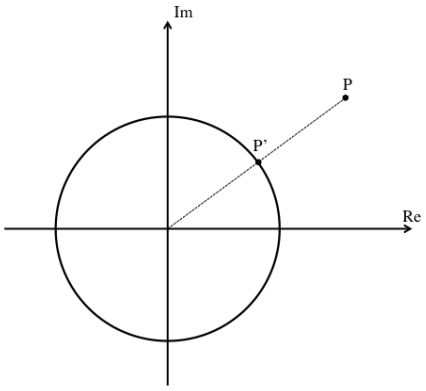

Figure 1. Unit circle on a complex plane. P' is a point on the circle, and P is a point to be optimized.

4. Evaluation

4.1. Hologram calculation and far field diffraction simulation

We tested our algorithm by using a light field image captured by a Lytro Illum camera, as shown in Figure 2.

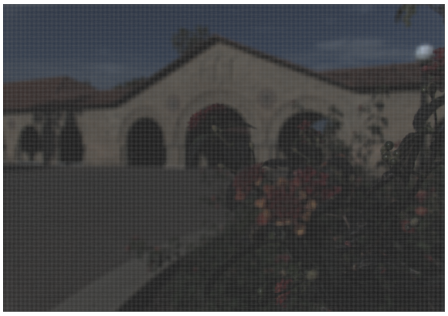

Figure 2. Rectified light field from Lytro Illum provided by Professor Wetzstein.

We calculated the target wavefront as described above. The magnitude and phase are shown in Figure 3 and Figure 4, respectively. The focal length is estimated to be $25\mu m$ based on the previous Lytro specifications, as the Illum microlens details have not yet been released. However the pixel pitch, $1.4\mu m$ is available and much more important to the calculations. The magnitude of this complex field is dark and has lines, which may suggest the focal length estimate is a little off. There is no information that can be directly seen from the calculated phase of the image.

We use the optimization algorithm to create a Fourier hologram that best approximates the complex matrix in the far field. The phase of the hologram is shown in Figure

Figure 3. Magnitude of Wigner calculated complex wave information.

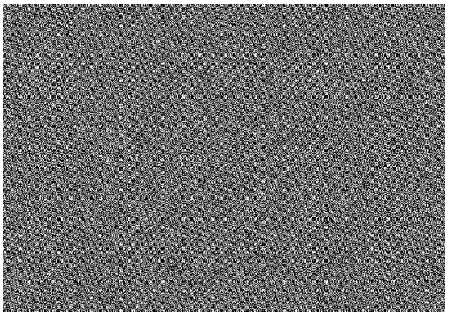

Figure 4. Phase of Wigner calculated complex wave information.

5, with grayscale equating to a delay of 0 to 2π. This hologram is what will be directly shown on the PLUTO phase-only LCoS SLM to test the direct view.

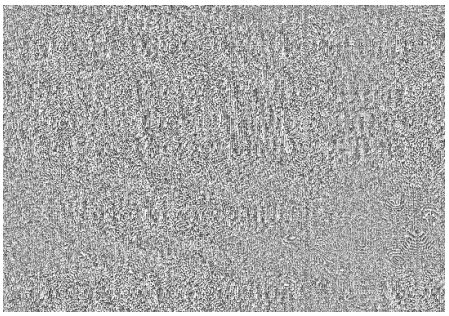

Figure 5. Fourier phase only hologram optimized from Wigner extracted complex matrix

We use the FFT to simulate the image in the far field, as shown in Figure 6. Many of the resulting holograms had a large DC spike in the center, so that to see the church image we had to brighten after normalization. We indicated the extent of brightening and contrast correction where needed.

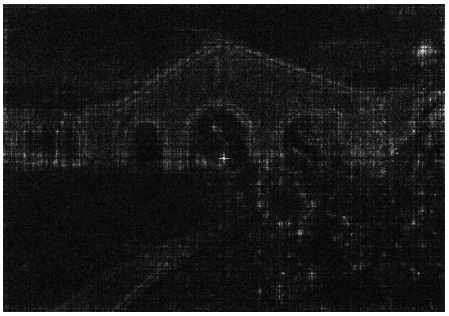

Figure 6. Far field diffraction of the optimized Fourier hologram using FFT. It has been brightened by 4x.

In an attempt to lessen the saturation in the middle as well as the patchiness, we subject the input complex matrix to a gaussian blur (σ=0.5), as well as enhance the contrast of the magnitude. The resulting input magnitude (Figure 7), calculated Fourier hologram (Figure 8) and far-field diffraction (Figure 9) are shown below. This hologram will be used on the PLUTO SLM to demonstrate far field projection.

Figure 7. Magnitude of blurred and contrast corrected complex wave information.

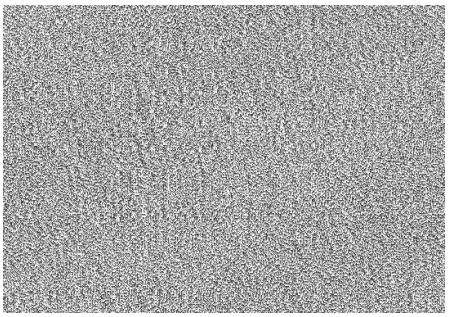

Figure 8. Fourier phase only hologram optimized from blurred complex matrix

Figure 9. Far field diffraction of the blurred Fourier hologram using FFT. It has been brightened by 4x

Additionally, we checked that the optimization of a non-complex image, specifically the (7, 7) perspective from the light field, does not work as well. Figures 10, 11, and 12 show the magnitude, phase-only hologram, and the far-field diffraction of the (7, 7)-perspective non-complex image, respectively. This test helps to show that the Wigner-distribution-extracted information is in fact useful. We can see within the hologram (Figure 11) that the phase of the higher spatial frequencies become blurred compared to the previous holograms, which we believe demonstrates the added information of the light field. This hologram did not work at all when testing direct view or projection.

Figure 10. Magnitude of the (7,7), center of microlens pixels only.

Finally, we evaluate our optimization routine by comparing it to a phase hologram calculated only from the phase of the Fourier transform of the target matrix. The input is the blurre, contrast enhanced complex matrix U, and the hologram is calculated using only the phase of the fourier transform of U. The resulting hologram is shown (Figure 13) along with its calculated far field diffraction (14). Although it is hard to compare this result to the optimized result using the calculated far field diffration, the actual projection and direct view of this hologram was much worse than the optimized hologram. Our camera was unable to capture the hologram, and so we can infer that the optimization algorithm produces a better algorithm than just taking the phase of the Fourier transform.

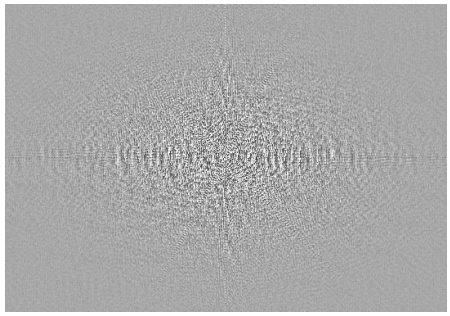

Figure 11. Fourier phase only hologram from non-complex image.

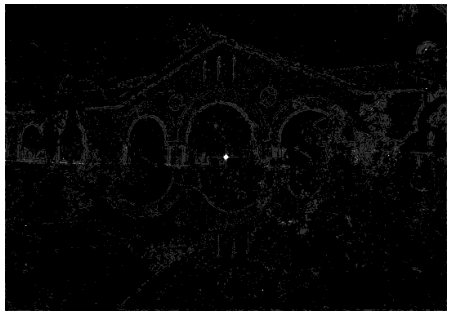

Figure 12. Far field diffraction of the non-complex image Hologram. Brightening and contrast correction was done in GIMP 2.0, with both set to 128.

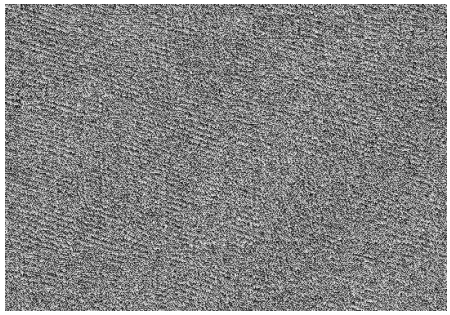

Figure 13. Non-optimized Fourier hologram.

4.2. Projection and direct view of calculated holograms

We tested the holograms using a PLUTO SLM. The setup also included a laser source, two lenses acting as a beam expander before the PLUTO, and two lenses acting as a relay system after the PLUTO, as shown in Figure

Figure 14. Far field diffraction of the non-optimized Hologram.

15. The relay system is setup so that the Fourier transform of the PLUTO is shown in the far field. In this case, we project the light onto the ceiling (Figures 16 and 17) in order to see the original image. Alternatively, a camera or eye placed a focal distance away from the focus of the second lens will also see the image. We call this configuration direct view of the hologram. Images captured by a Canon Powershot are included, though real-life viewing is much better. The less than 100% fill factor results in an amplitude grating at half the period of the pixel pitch, which causes the image to diffract into the multiple orders scene as well as the bright DC artifact in the center of the image. Prefiltering the light may improve the image quality.

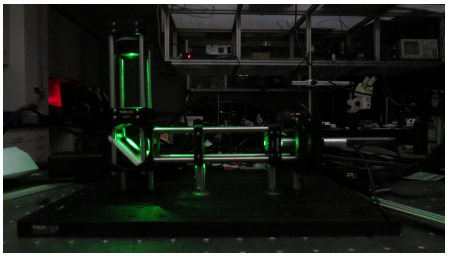

Figure 15. Optical setup. The laser is 532nm, the bottom two lenses expand the laser beam, the PLUTO is mounted on a 3D printed holder, the bottom relay lens has a focal length of 60mm and the top relay lens has a focal length of 25mm.

4.3. The Final Presentation Demo

It is important to note that the demonstration given for the presentation was using a different method to calculate the holograms. The ones displayed that day were not Fourier holograms, but directly imaged from the PLUTO using a phase grating scheme, shown in Figure 19. This demonstration was based on Stephen's previous work in attempting to emulate the Grating Light Valve, a phase and amplitude modulator, using the PLUTO. Multiple PLUTO

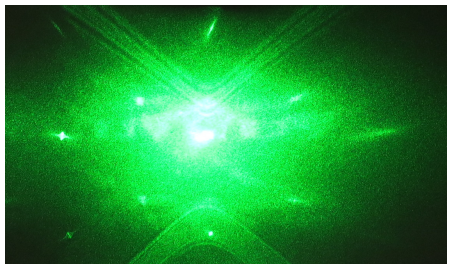

Figure 16. Projection of the hologram onto the ceiling. The multiple orders and the bright spot are artifacts of the pixel fill factor of the PLUTO.

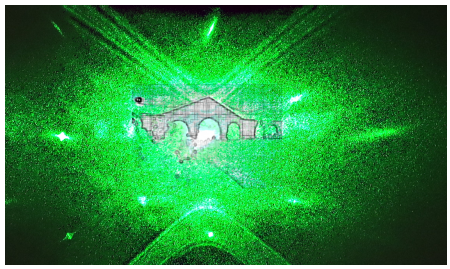

Figure 17. Far field simulation overlayed onto the holographic projection.

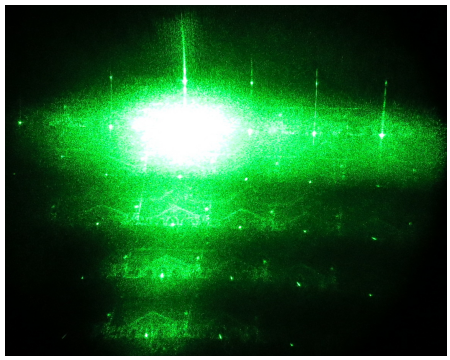

Figure 18. Direct view of the hologram. A ND filter is used to protect the camera and the eyes.

pixels are required per holographic pixel (holopixel) as well as a 4π phase stroke. For a given $\theta 1$ and $\theta 2$, when the DC orders are blocked, the average of the reconstructed, blurred orders result in a holopixel of complex value C such that:

$$C = \cos\frac{\theta 1 - \theta 2}{2} \exp i\frac{\theta 1 + \theta 2}{2} \tag{15}$$

Therefore, given a desired amplitude and phase, the required grayvalues of the grating is easily calculated. For the demo, we used a simple 2x2 grating in the vertical direction.

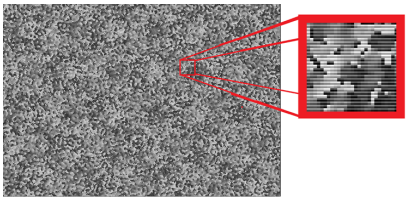

Figure 19. Hologram used in final presentation demo. Note that this hologram is filtered in the Fourier plane and then viewable within the original plane.

We do not have a picture of the demonstration hologram at this time.

5. Discussion

We have demonstrated that we can utilize the additional information provided by a light field recording to construct a phase-only Fourier hologram. Observing the hologram confirms that the optimized hologram from the Wigner-distribution-produced complex matrix produced the best reconstruction of the light field image, though increasing the contrast of the image helped. Unfortunately, we were unable to verify the depth effects of the hologram. Better optics as well as complete information of the Illum's specifications may enable us to improve upon the display. Additionally, another object could be selected that would better demonstrate the depth cues of the hologram.

At this point, it is prudent to discuss the relationship between the coherent hologram and the incoherent light field. At first, transforming from an incoherent field to a coherently lit scene may seem troublesome. However, two facts must be kept in mind to realize that this transformation is valid. First, we are merely comparing the Wigner of the coherently lit PLUTO in an attempt to reconstruct the light field scene, and so an exact equivalence is unnecessary. In fact, it would be better to optimize by calculating the Wigner distribution of the PLUTO, and then blurring and sampling it to compare it to the light field recording. However, the Wigner distribution is a non-linear function and so this optimization may prove to be more difficult and computationally intensive. Second, the light field is a geometric optics model. Therefore, we are only interested in the direction and position of the ray of light that is striking the pixel. We then apply this directionality to a plane wave and are thus able to treat the resulting Wigner as a Fourier model.

6. Future Work

Additional work can be done to improve the algorithm, especially attempting the Wigner optimization mentioned in the discussion. However, improved technology is necessary for both the optimal recording of a light field as well as light modulation for holographic display. For the light field recording, smaller and more numerous pixels are necessary in order to better sample the incoming light rays' directionality. Greater sampling will improve resolution of the spatial frequencies of the hologram, allowing for finer depth perception. Eric Fossum has discussed a digital film that uses tiny pixels called jots [5]. This technology may have promising use in light field as well as traditional interferometric recording for holographic purposes. On the display side, research into combine phase and amplitude modulators as well as nano-wire displays could make wearable holographic displays a reality.

7. References

References

[1] Ziegler, R., Bucheli, S., Ahrenberg, L., Magnor, M. and Gross, M. (2007), "A Bidirectional Light Field - Hologram Transform," Computer Graphics Forum, 26: 435-446. doi: 10.1111/j.1467-8659.2007.01066.x

[2] Zhang, Z., Levoy, M. (2009), "Wigner Distributions and How They Relate to the Light Field," 2009 IEEE International Conference on Computational Photography (ICCP): 1-10. doi: 10.1109/ICCPHOT.2009.5559007

[3] Goodman, J. (2013), "Holography Viewed from the Perspective of the Light Field Camera," Fringe 2013, pp3-15. Springer Berlin Heidelberg.

[4] Lohmann, A., Testorf, M. and Ojeda-Castaneda, J. (2002), "Holography and the Wigner Function," Proc. SPIE 4737, Holography: A Tribute to Yuri Denisyuk and Emmett Leith, 77. doi:10.1117/12.474960

[5] Fossum, E. (2014), "Quanta Image Sensor (QIS) Concept and Progress," SCIEN Talk. https://scien.stanford.edu/index.php/professor-eric-fossum/